Chlorido(4,4′-dimethoxy-2,2′-bipyridine)(1,4,7-trimethyl-1,4,7-triazacyclononane)ruthenium(II) perchlorate acetonitrile disolvate and aqua(4,4′-dimethoxy-2,2′-bipyridine)(1,4,7-trimethyl-1,4,7-triazacyclononane)ruthenium(II) bis(perchlorate) dihydrate

Daniela B. Vera, Nicolás Osa Codesido, Ariel G. De Candia, Pablo Alborés* and Leonardo D. Slep*

INQUIMAE–DQIAyQF–Universidad de Buenos Aires, Ciudad Universitaria, Pab. 2, piso 3, (C1428EHA) Buenos Aires, Argentina

Correspondence e-mail: albores@qi.fcen.uba.ar, slep@qi.fcen.uba.ar

The title complexes, $[RuCl(C_9H_{21}N_3)(C_{12}H_{12}N_2O_2)]ClO_4\cdot 2C_2H_3N$, (I), and $[Ru(C_9H_{21}N_3)(C_{12}H_{12}N_2O_2)(H_2O)](ClO_4)_2\cdot 2H_2O$, (II), display similar structures with the Ru atom in a distorted octahedral environment. In the crystal packing of the chloride complex, (I), the Ru complex molecules are held together in pairs through C—H···Cl interactions of the 4,4′-dimethoxy-2,2′-bipyridine and chloride ligands. In the case of the aqua complex, (II), hydrogen bonding affords a tetrameric hydrogen-bonded network. These two structures are the first examples of complexes with the {Ru(1,4,7-trimethyl-1,4,7-triazacyclononane)} motif and an electron-rich substituted 2,2′-bipyridine ligand.

Comment

Ruthenium(II)–tmtacn (tmtacn = 1,4,7-trimethyl-1,4,7-triazacyclononane) complexes containing aromatic diimine ligands such as 2,2′-bipyridine (bpy) and 1,10-phenanthroline (phen) are of considerable interest in catalysis, including a large number of reactions such as epoxidation of alkenes, oxidation of alkanes, alcohols, aldehydes and arenes, oxidative cleavage of C═C and C—C bonds, cis-dihydroxylation of alkenes, and amination of saturated C—H bonds (Chan et al., 2011). Tuning of the redox potential of the metal-centred processes is a key issue in the design of these catalysis reagents in order to facilitate access to high Ru oxidation states. In this sense, modification of the electronic properties of the co-ligands has become the preferred approach of working on this problem.

The synthesis of $[Ru(bpy)(tmtacn)(H_2O)](ClO_4)_2$ was reported several years ago by Cheng et al. (1994). The preparation involves the reaction under reflux between stoichiometric amounts of $Ru(tmtacn)Cl_3$ and bpy in water in the presence of Zn^0. We followed this strategy to prepare and crystallize the analogue $[Ru(tmtacn)\{4,4′-(MeO)_2bpy\}(H_2O)](ClO_4)_2\cdot 2H_2O$, (II), bearing the electron-rich bpy derivative 4,4′-dimethoxy-2,2′-bipyridine $[4,4′-(MeO)_2bpy]$. A serendipitous event, viz. the accidental contamination of a crystallization flask with NaCl, allowed us to obtain and crystallize the chloro derivative $[RuCl(tmtacn)\{4,4′-(MeO)_2bpy\}]ClO_4\cdot 2CH_3CN$, (I).
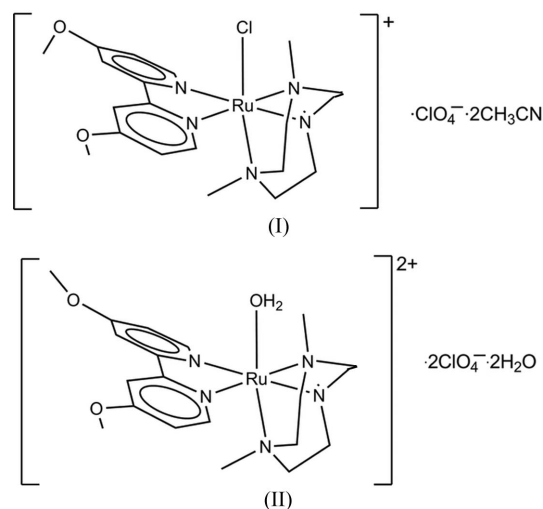

Complex (I) crystallizes in the monoclinic $C2/c$ space group, with one perchlorate counter-ion and two acetonitrile solvent molecules in the asymmetric unit, whereas complex (II) crystallizes in the triclinic $P\bar{1}$ space group with two perchlorate counter-ions and two water solvent molecules in the asymmetric unit. With respect to the coordination sphere of the metal centre, complexes (I) and (II) display similar structures (Figs. 1 and 2, respectively). The coordination geometry around the Ru atom in each case is distorted octahedral. As expected, the tmtacn ligand coordinates in a facial manner to
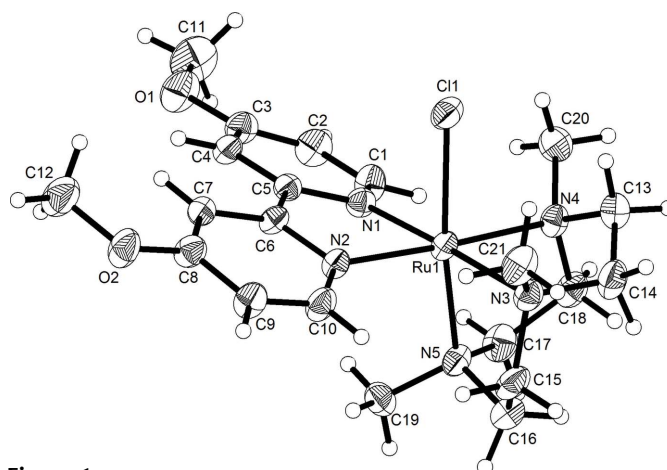
Figure 1
Displacement ellipsoid plot of the complex cation of (I), with ellipsoids drawn at the 30% probability level.
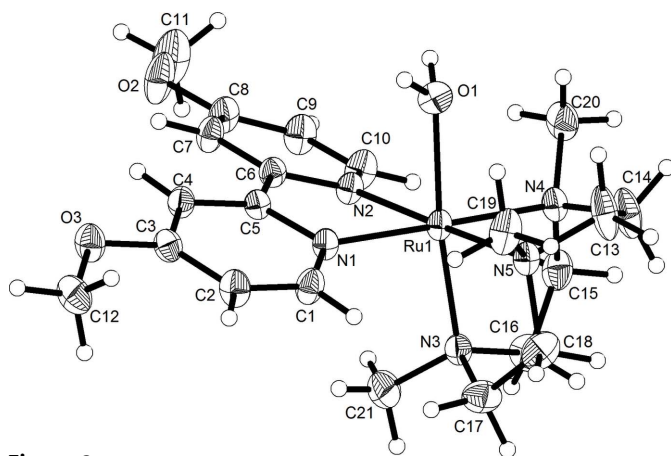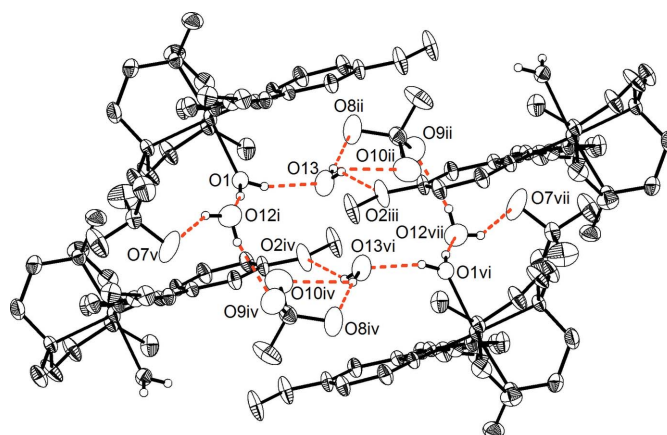
Figure 2
Displacement ellipsoid plot of the complex cation of (II), with ellipsoids drawn at the 30% probability level.
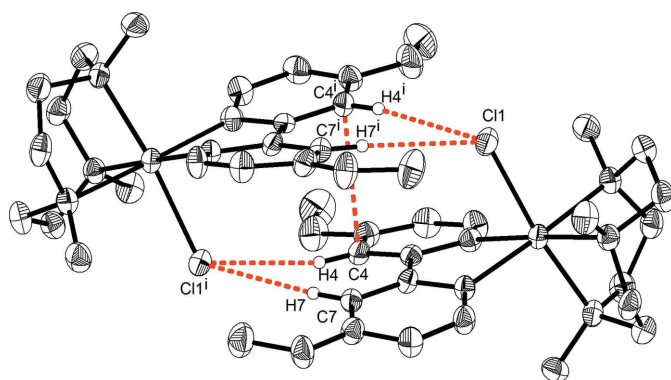
Figure 3
Displacement ellipsoid plot of the hydrogen-bond network in complex (I), with ellipsoids drawn at the 30% probability level. Only H atoms involved in the Cl···H—C interactions are shown. [Symmetry code: (i) $-x, y, -z + \frac{1}{2}$.]

Figure 4
Displacement ellipsoid plot of the short contact pair interactions in complex (II), with ellipsoids drawn at the 30% probability level. Only water H atoms are shown. [Symmetry codes as in Table 4; additionally: (vi) $-x, -y, -z$; (vii) $-x, -y + 1, -z$.]

the Ru atom with atom N5 *trans* to the chloride ligand in (I) and atom N3 *trans* to the O atom of the coordinated water ligand in (II). The bidentate 4,4′-(MeO)$_2$bpy ligand completes the octahedral environment. In (I), the Ru—Cl distance of 2.4343 (11) Å is slightly longer than that observed in the only other chloro-containing Ru^{II} complex with an {Ru(tmtacn)} moiety reported in the literature, namely [RuCl(tmtacn)-(CO)$_2$]PF$_6$ (Yang *et al.*, 1995), which features an Ru—Cl distance of 2.410 (2) Å. In (II), the Ru—O distance of 2.149 (4) Å is shorter than that observed in the bipyridine parent compound [Ru(tmtacn)(bpy)(H$_2$O)](ClO$_4$)$_2$ (Cheng *et al.*, 1994), with an Ru—O distance of 2.168 (3) Å. As a consequence, the *trans* N atom of the tmtacn ligand exhibits a larger Ru—N distance than that observed in the previously published analogue [2.103 (4) Å *versus* 2.087 (4) Å]. With respect to the *trans* N atom of tmtacn in complex (I), the presence of the donor chloride ligand affords an even longer Ru—N bond length of 2.121 (3) Å. The remaining donor N atoms of the tmtacn ligand in both complexes exhibit similar Ru—N bond lengths (Tables 1 and 3) that also agree with those observed in [Ru(bpy)(tmtacn)(H$_2$O)]$^{2+}$. A similar situation is observed for the Ru—N bond lengths of the

coordinated 4,4′-(MeO)$_2$bpy ligand. In the aqua complexes (II) and [Ru(bpy)(tmtacn)(H$_2$O)]$^{2+}$, the Ru—N bond lengths are statistically equivalent.

In both complexes, the planar 4,4′-(MeO)$_2$bpy ligand appears tilted with respect to the plane containing the N atoms of this ligand and the Ru centre, with dihedral angles of 16.85 (12) and 16.17 (18)° in (I) and (II), respectively. For the calculation of these angles, the plane containing the 12-membered ring (ten C and two N atoms) of 4,4′-(MeO)$_2$bpy and the plane containing the Ru atom together with the 4,4′-(MeO)$_2$bpy N atoms and the equatorial tmtacn ligand N atoms were considered. The tilting direction is toward the aqua and chloride ligands in these cases and it is most probably due to the steric hindrance caused by the methyl group from the tmtacn ligand. The same behaviour is observed in related complexes (Cheng *et al.*, 1994, 1996; Wong *et al.*, 2009).

In the crystal packing of (I), the Ru complex cations are held together in pairs through Cl···H—C interactions involving the coordinated chloride ligand and the 4,4′-(MeO)$_2$bpy ligand, with Cl···H—C contact distances of Cl1···H4($-x, y, -z + \frac{1}{2}$) = 2.65 Å and Cl1···H7($-x, y, -z + \frac{1}{2}$) = 2.77 Å. This affords an apparent stacking of the 4,4′-(MeO)$_2$bpy ligands, with the shortest C···C contact being C4···C4($-x, y, -z + \frac{1}{2}$) of 3.339 (5) Å (Fig. 3 and Table 2). The perchlorate counter-ion and the acetonitrile solvent molecules are also involved in short-contact interactions.

Regarding the crystal packing of (II), hydrogen-bonding interactions involving the O atoms of the coordinated water molecule, the O atoms of the 4,4′-(MeO)$_2$bpy and the O atoms of the solvent water molecules afford a tetrameric hydrogen-bonded network (Fig. 4). The hydrogen-bond interactions and distances are listed in Table 4.

Complexes (I) and (II) are the first examples of structurally characterized ruthenium fragments bearing the {Ru(bpy)-(tmtacn)}$^{2+}$ motif with an electron rich bpy-type ligand. Moreover, the chloro derivative is only the second reported structure of an Ru^{II} complex with the general motif {Ru(tm-tacn)} and containing any Ru—Cl bond. Both appear to be

promising ruthenium complexes to explore their high-oxidation-state derivatives and their potential catalysis capability.

Experimental

For the synthesis of (I), [Ru(tmtacn)]Cl$_3$·H$_2$O (100.5 mg, 0.25 mmol; Neubold *et al.*, 1989), 4,4′-dimethoxy-2,2′-bipyridine (81.3 mg, 0.38 mmol) and Zn/Hg (150 mg) were suspended in H$_2$O (20 ml) and refluxed for 1 h under an argon atmosphere. The reactants dissolved slowly to yield a pale-green solution which during the course of the reaction became deeply burgundy. At this point the insolubles were removed from the reaction mixture by filtration and the solution was concentrated on a rotary evaporator to a volume of less than 5 ml. Addition of NaClO$_4$ (600 mg, 4.90 mmol) induced the precipitation of the product as a fine powder, which after standing overnight in a refrigerator was collected by filtration, washed with chilled water and dried over silica gel. A small amount of a white material (most likely an excess of the ligand) was removed with diethyl ether. The deeply coloured material was finally dissolved in water and allowed to evaporate slowly at room temperature to yield 153 mg (80%) of the product. The material obtained in this way was suitable for X-ray analysis.

Table 1
Selected interatomic distances (Å) for (I).

Cl1—Ru1	2.4343 (11)	N3—Ru1	2.164 (3)
N1—Ru1	2.081 (3)	N4—Ru1	2.161 (3)
N2—Ru1	2.091 (3)	N5—Ru1	2.121 (3)
C4···C4^i	3.339 (5)		

Symmetry code: (i) $-x, y, -z + \frac{1}{2}$.

Table 2
Hydrogen-bond geometry (Å, °) for (I).

D—H···A	D—H	H···A	D···A	D—H···A
C4^i—H4^i···Cl1	0.93	2.65	3.562 (4)	167
C7^i—H7^i···Cl1	0.93	2.77	3.695 (4)	176

Symmetry code: (i) $-x, y, -z + \frac{1}{2}$.

Table 3
Selected bond lengths (Å) for (II).

N1—Ru1	2.089 (3)	N4—Ru1	2.154 (3)
N2—Ru1	2.106 (3)	N5—Ru1	2.148 (3)
N3—Ru1	2.104 (4)	O1—Ru1	2.151 (3)

Table 4
Hydrogen-bond geometry (Å, °) for (II).

D—H···A	D—H	H···A	D···A	D—H···A
O1—H1W···O12^i	0.82 (3)	1.96 (4)	2.751 (6)	161 (5)
O1—H2W···O13	0.82 (2)	1.94 (2)	2.729 (5)	162 (6)
O13—H3W···O8^{ii}	0.93 (4)	2.39 (4)	3.314 (7)	175 (5)
O13—H3W···O10^{ii}	0.93 (4)	2.46 (5)	3.112 (7)	128 (4)
O13—H4W···O2^{iii}	0.81 (4)	2.28 (4)	2.936 (6)	138 (3)
O12^i—H5W···O9^{iv}	0.84 (5)	2.13 (5)	2.945 (7)	164 (5)
O12^i—H6W···O7^v	0.83 (2)	2.46 (5)	3.126 (7)	138 (5)

Symmetry codes: (i) $x, y - 1, z$; (ii) $-x + 1, -y + 1, -z$; (iii) $-x + 1, -y, -z$; (iv) $x - 1, y - 1, -z + 1$; (v) $-x + 1, -y, -z + 1$.

For the preparation of (II), a solution of [Ru(tmtacn){4,4′-(MeO)$_2$bpy}(H$_2$O)](ClO$_4$)$_2$·2H$_2$O in water originally intended to be used to grow large single crystals was accidentally contaminated with NaCl. Complete evaporation of the solvent yielded a red material, which was suspended in acetonitrile and filtered to remove insoluble inorganic salts. Slow diffusion of diethyl ether yielded red single crystals that turned out to be compound (II).

Compound (I)

Crystal data

[RuCl(C$_9$H$_{21}$N$_3$)(C$_{12}$H$_{12}$N$_2$O$_2$)]-ClO$_4$·2C$_2$H$_3$N	$\beta = 98.603$ (6)°
$M_r = 705.60$	$V = 6207.6$ (6) Å^3
Monoclinic, $C2/c$	$Z = 8$
$a = 17.8073$ (9) Å	Mo $K\alpha$ radiation
$b = 12.3587$ (7) Å	$\mu = 0.73$ mm^{-1}
$c = 28.5276$ (18) Å	$T = 298$ K
	$0.38 \times 0.28 \times 0.12$ mm

Data collection

Oxford Diffraction Xcalibur Eos Gemini diffractometer	13768 measured reflections
Absorption correction: multi-scan (*CrysAlis PRO*; Oxford Diffraction, 2010)	6674 independent reflections
	3528 reflections with $I > 2\sigma(I)$
$T_{min} = 0.816$, $T_{max} = 1.000$	$R_{int} = 0.051$

Refinement

$R[F^2 > 2\sigma(F^2)] = 0.047$	30 restraints
$wR(F^2) = 0.122$	H-atom parameters constrained
$S = 0.87$	$\Delta\rho_{max} = 0.59$ e Å^{-3}
6674 reflections	$\Delta\rho_{min} = -0.42$ e Å^{-3}
372 parameters	

Compound (II)

Crystal data

[Ru(C$_9$H$_{21}$N$_3$)(C$_{12}$H$_{12}$N$_2$O$_2$)-(H$_2$O)](ClO$_4$)$_2$·2H$_2$O	$\beta = 96.740$ (7)°
$M_r = 741.54$	$\gamma = 103.386$ (8)°
Triclinic, $P\bar{1}$	$V = 1487.4$ (2) Å^3
$a = 8.1705$ (6) Å	$Z = 2$
$b = 10.3825$ (11) Å	Mo $K\alpha$ radiation
$c = 18.1967$ (15) Å	$\mu = 0.78$ mm^{-1}
$\alpha = 92.464$ (7)°	$T = 298$ K
	$0.30 \times 0.12 \times 0.05$ mm

Data collection

Oxford Diffraction Xcalibur Eos Gemini diffractometer	18945 measured reflections
Absorption correction: multi-scan (*CrysAlis PRO*; Oxford Diffraction, 2010)	6429 independent reflections
	4889 reflections with $I > 2\sigma(I)$
$T_{min} = 0.946$, $T_{max} = 1.000$	$R_{int} = 0.078$

Refinement

$R[F^2 > 2\sigma(F^2)] = 0.053$	H atoms treated by a mixture of independent and constrained refinement
$wR(F^2) = 0.144$	
$S = 1.03$	
6429 reflections	$\Delta\rho_{max} = 1.17$ e Å^{-3}
397 parameters	$\Delta\rho_{min} = -1.00$ e Å^{-3}
11 restraints	

In both structures, all C-bound H atoms were clearly visible in a difference Fourier map, but in the refinement they were repositioned at their expected locations and allowed to ride, with C—H = 0.93 (aromatic), 0.96 (methyl) and 0.97 Å (methylene). For the O—H and

metal-organic compounds

methyl H atoms, $U_{iso}(H) = 1.5U_{eq}$(parent atom), while $U_{iso}(H) = 1.2U_{eq}$(parent atom) for all other H atoms.

In (I), in order to make the refinement of the acetonitrile solvent molecules fully anisotropic, all their C and N atoms were subjected to a 'rigid bond' restraint (DELU instruction in *SHELXL97*; Sheldrick, 2008), *i.e.* the components of the (anisotropic) displacement parameters in the direction of the corresponding bonds were restrained to be equal within an effective standard uncertainty of 0.02 Å. In addition, within this same set of atoms, those closer than 1.7 Å were restrained with an effective standard uncertainty of 0.04 Å to have the same U^{ij} components (SIMU instruction).

In (II), coordinated water H atoms were located in a difference Fourier map and positioned accordingly. The H atoms of the solvent water molecules were not located in the difference map but were positioned geometrically using the CALC-OH algorithm (Nardelli, 1999). H atoms attached to O atoms were refined with restrained O—H distances of 0.84 (2) Å and the water H···H distances were restrained to 1.30 (4) Å.

The refinement of the H atoms of the solvent water molecules in (II) required the inclusion of some intermolecular restraints to avoid convergence to unreasonable intermolecular H···H distances. The H···O intermolecular shortest contact distances were restrained to 2.30 (2) Å. In this way, refinement converged to a reasonable hydrogen-bonded network although no significant improvement in the overall statistics was achieved.

For both compounds, data collection: *CrysAlis PRO* (Oxford Diffraction, 2010); cell refinement: *CrysAlis PRO*; data reduction: *CrysAlis PRO*; program(s) used to solve structure: *SHELXS97* (Sheldrick, 2008); program(s) used to refine structure: *SHELXL97* (Sheldrick, 2008); molecular graphics: *WinGX* (Farrugia, 1999); software used to prepare material for publication: *DIAMOND* (Crystal Impact, 1999).

References

Chan, S. L. F., Kan, Y. H., Yip, K. L., Huang, J. S. & Che, C. M. (2011). *Coord. Chem. Rev.* **255**, 899–919.

Cheng, W. C., Yu, W. Y., Cheung, K. K. & Che, C. M. (1994). *J. Chem. Soc. Dalton Trans.* pp. 57–62.

Cheng, W. C., Yu, W. Y., Zhu, J., Cheung, K. K., Peng, S. M., Poon, C. K. & Che, C. M. (1996). *Inorg. Chim. Acta*, **242**, 105–113.

Crystal Impact (1999). *DIAMOND*. Crystal Impact GbR, Bonn, Germany.

Farrugia, L. J. (1999). *J. Appl. Cryst.* **32**, 837–838.

Nardelli, M. (1999). *J. Appl. Cryst.* **32**, 563–571.

Neubold, P., Dellavedova, B., Wieghardt, K., Nuber, B. & Weiss, J. (1989). *Angew. Chem. Int. Ed. Engl.* **28**, 763–765.

Oxford Diffraction (2010). *CrysAlis PRO*. Oxford Diffraction Ltd, Yarnton, Oxfordshire, England.

Sheldrick, G. M. (2008). *Acta Cryst.* A**64**, 112–122.

Wong, C. Y., Lai, L. M., Leung, H. F. & Wong, S. H. (2009). *Organometallics*, **28**, 3537–3545.

Yang, S. M., Cheng, W. C., Peng, S. M., Cheung, K. K. & Che, C. M. (1995). *J. Chem. Soc. Dalton Trans.* pp. 2955–2959.